Normal modes of tetragonal $YBa_2Cu_3O_6$ and orthorhombic $YBa_2Cu_3O_7$

Frances E. Bates
Department of Physics, University of British Columbia, Vancouver, British Columbia, Canada V6T 2A6
(Received 29 August 1988)

Normal-coordinate calculations of the frequencies and form of the zero wave-vector vibrations of tetragonal $YBa_2Cu_3O_6$ and orthorhombic $YBa_2Cu_3O_7$ have been performed. The results are used to predict differences in the vibrational spectra of the semiconducting O_6 compound and the superconducting O_7 compound and are related to the observed infrared and Raman spectra. The calculations indicate that the 435-cm^{-1} Raman feature is not due to a first order A_g mode and that the anomalous behavior of the 310-cm^{-1} infrared mode is due in part to the Evans effect.

There has been considerable interest lately in the effect of oxygen stoichiometry on the vibrational spectra of $YBa_2Cu_3O_{7-x}$.[1-13] Infrared spectra[1-5] of superconducting orthorhombic $YBa_2Cu_3O_7$ exhibit a sparcity of vibrational features. Although there are 21 predicted infrared active modes, only six infrared vibrational features have been clearly identified. In contrast, for the semiconducting tetragonal $YBa_2Cu_3O_6$ where there are eleven predicted infrared active modes, at least nine infrared vibrational features have been observed.[6,7] Raman spectra[4,5,7-14] of both the superconducting and semiconducting compounds exhibit only six well-identified features compared with the fifteen predicted for the orthorhombic form and the ten for the tetragonal form.

The origin of the observed vibrational features is the subject of much debate. A number of lattice-dynamical calculations have been reported lately for the orthorhombic form[2,15-18] and for the tetragonal form[7,8] which have yielded descriptions of the normal modes and phonon densities of states. Normal-coordinate calculations, which are applicable to zero wave-vector normal-mode analysis, have the advantage over lattice-dynamical calculations in that noncentral forces such as those involved in angle bending can be readily treated. Normal-coordinate calculations have been used extensively for other metal oxides[19] and have greatly aided in their vibrational analysis. The importance of angle-bending force constants is proportional to the covalency of the compound[20] and clearly for the copper-oxygen framework of these systems, with an estimated covalency[21] of 0.5, they should be considered.

A preliminary normal-coordinate calculation of orthorhombic $YBa_2Cu_3O_7$ has been reported.[22] Those calculations have now been extended to the tetragonal compound and, using new infrared and Raman data, have allowed a detailed assignment of the vibrational features of both the orthorhombic and the tetragonal materials.

The orthorhombic unit cell of the superconducting $YBa_2Cu_3O_7$ is shown in Fig. 1, the numbering of the atoms is the same as used previously.[22] The space group is $Pmmm(D_{2h}^1)$.[23] Three atoms, Cu(1), Y, and O(1), sit on sites of symmetry D_{2h}, while the remaining atoms, Cu(2), Ba, O(2), O(3), and O(4), sit on sites of symmetry C_{2v}. The thirteen atoms of the unit cell yield a total of 36 vibrational modes forming the irreducible representation

$$\Gamma = 5A_g + 5B_{2g} + 5B_{3g} + 7B_{1u} + 7B_{2u} + 7B_{3u} .$$

The tetragonal unit cell of the semiconducting $YBa_2Cu_3O_6$ (Ref. 1) is essentially the same as that given in Fig. 1, except that O(1) is absent and the twofold rotation axis parallel to the c axis becomes a fourfold axis, making O(3) and O(4) equivalent. Cu(1) and Y then occupy sites of symmetry D_{4h}; Cu(2), Ba, and O(2) occupy sites of symmetry C_{4v}; and O(3) and O(4) occupy sites of symmetry C_{2v}. The twelve atoms of the unit cell yield a total of 33 vibrational modes:

$$\Gamma = 4A_{1g} + B_{1g} + 5E_g + 5A_{2u} + B_{2u} + 6E_u .$$

For the orthorhombic form the Raman-active modes are of type A_g, B_{2g}, and B_{3g} while for the tetragonal form they are of type A_{1g}, B_{1g}, and E_g. Thus, there are fifteen Raman active modes for the orthorhombic form and ten for the tetragonal form. The infrared active modes are of type B_{1u}, B_{2u}, and B_{3u} for the orthorhombic form and of type A_{2u} and E_u for the tetragonal form; the B_{2u} mode being inactive in the tetragonal form. There are, therefore, 21 infrared-active modes in the orthogonal form and eleven in the tetragonal form.

The correlation of the normal modes of the tetragonal form to those of the orthorhombic form is given in Table I. (This table will be discussed in greater detail below.) For the Raman active modes, the four A_{1g} modes and one B_{1g} mode of the tetragonal form yield the A_g vibrations of the orthorhombic form, while each of the five doubly degenerate E_g vibrations of the tetragonal form yields a B_{2g} mode and a B_{3g} mode for the orthorhombic form. Thus,

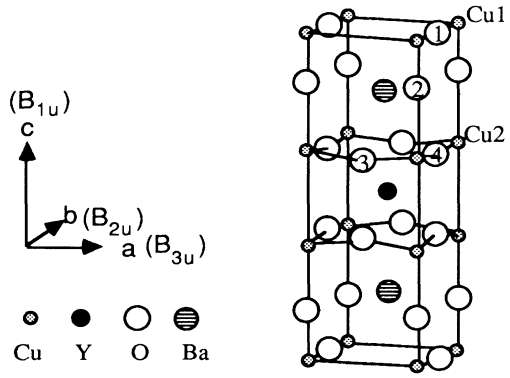

FIG. 1. Orthorhombic unit cell of $YBa_2Cu_3O_7$.

TABLE I. Calculated and observed[a] frequencies for $YBa_2Cu_3O_7$ and $YBa_2Cu_3O_6$.

PED[b] $YBa_2Cu_3O_7$	Mode	υ_{obs}	υ_{cal}	υ_{cal}	υ_{obs}	Mode	PED $YBa_2Cu_3O_6$
$0.70C_2+0.51C_4-0.18i_2$	A_g	502	502	→491	479	A_{1g}	$0.59C_2+0.38C_4-0.19i_3$
$0.61B_3+0.43Y-0.16i_3$	A_g	435?	352	→349	455?	A_{1g}	$0.55B_3+0.38Y-0.16i_3$
$0.57B_3+0.53Y-0.17i_3$	A_g	340	332	→331	341	B_{1g}	$0.60B_3+0.53Y-0.17i_3$
$0.52CC+0.19C_2+0.15C_4$	A_g	230	222	→220	220	A_{1g}	$0.56CC+0.19C_4+0.19C_2$
$0.45B_1+0.25Y+0.16B_3$	A_g	151	126	→135	141	A_{1g}	$0.50BB+0.24Y$
$0.91C_3$	B_{2g}		647	→642		E_g	$0.89C_3$
$0.88C_3$	B_{3g}		635				
$0.49\alpha+0.34Y$	B_{3g}		534	→535		E_g	$0.48\alpha+0.33Y+0.16B_3$
$0.48\alpha+0.32Y$	B_{2g}		532				
$0.63B_2+0.37\alpha$	B_{3g}		463				
$0.99B_2$	B_{2g}		367	→ 365	390	E_g	$0.99B_2$
$0.42B_3+0.34\alpha+0.21Y$	B_{3g}	115	123	→119		E_g	$0.42\alpha+0.34B_3+0.33Y$
$0.38B_3+0.34\alpha+0.24Y$	B_{2g}	115	121				
$0.35Y+0.29\alpha+0.16B_2$	B_{3g}		92	→62		E_g	$0.51B_3+0.35Y$
$0.48B_1+0.30Y$	B_{2g}		90				
$0.61C_2+0.19\alpha+0.17C_4$	B_{1u}	609	611	→606	593	A_{2u}	$0.77C_2+0.23C_4$
$0.38\alpha+0.36B_1+0.16C_2$	B_{1u}	548	531				
$0.62Y+0.46B_3-0.17i_3$	B_{1u}	310?	373	→371	360	A_{2u}	$0.64Y+0.47B_3-0.17i_3$
$0.59B_3+0.54Y-0.17i_3$	B_{1u}	310?	332	→331	i.a.	B_{2u}	$0.51B_3+0.45Y$
$0.59C_4+0.15B_1$	B_{1u}	279	255	→235	249	A_{2u}	$0.73C_4$
$0.47B_3+0.33Y$	B_{1u}	191	182	→181	190	A_{2u}	$0.49B_3+0.36Y$
$0.40\alpha+0.24B_1$	B_{1u}		111	→73	108	A_u	$0.34B_2+0.33C_3+0.29\alpha$
$0.95C_1$	B_{2u}		646				
$0.90C_3$	B_{3u}		647	→643	648	E_u	$0.88C_3$
$0.87C_3$	B_{2u}		636				
$0.43\alpha+0.37Y$	B_{2u}		544	→546	593	E_u	$0.43\alpha+0.38Y$
$0.44\alpha+0.40Y$	B_{3u}		543				
$0.55B_2+0.40\alpha$	B_{2u}		473	→400		E_u	$0.82B_2+0.18\delta$
$0.51B_2+0.25B_1+0.23\delta$	B_{3u}		407				
$0.42B_1+0.32B_2+0.26\alpha$	B_{3u}		382				
$0.61Y+0.32\alpha$	B_{2u}		187	→187	217	E_u	$0.61Y+0.34\alpha$
$0.60Y+0.34\alpha$	B_{3u}		187				
$0.52\alpha+0.38B_2$	B_{2u}	151	163	→125	147	E_u	$0.60\delta+0.24B_2$
$0.69\delta+0.20B_1+0.15B_2$	B_{3u}	151	154				
$0.81B_3$	B_{2u}		90	→88	118	E_u	$0.62B_2+0.21\delta$
$0.83B_3$	B_{3u}		89				

[a]The observed frequencies are from Refs. 1, 6, 10, and 11. Those observed features whose assignment is uncertain are indicated with a question mark.

[b]See Table II for the identification of the force constants.

apart from the possible splitting of the E_g vibrations and a possible change in the polarization of the B_{1g} mode, there should not be any dramatic differences in the Raman spectra of the orthorhombic and tetragonal forms.

For the infrared spectra the five infrared active A_{2u} modes and one infrared-inactive B_{2u} mode of the tetragonal form become six of the seven B_{1u} vibrations of the orthorhombic form, while each of the six doubly degenerate E_u vibrations yields a B_{2u} and a B_{3u} mode in the orthorhombic form. The additional oxygen [O(1)] in the orthorhombic material results in three additional modes (B_{1u}, B_{2u}, and B_{3u}). Thus, to a first approximation, the differences in the infrared spectra of the materials are that for the orthorhombic form there is a possible splitting of the E_u modes and the appearance of four new features, three due to O(1) and one due to the activation of the tetragonal B_{2u} mode.

The normal-coordinate calculations were done using Wilson's *GF* matrix method.[24] Initially, a simple valence-bond force field was adopted, consisting of bond-stretching and angle-bending coordinates. The types of force constant used and the types of internal-displacement coordinates to which they correspond are given in Table II. For the tetragonal form, the force field involves eight bond-stretching force constants and two types of angle-bending force constants (α and δ). For perovskite materials Saine, Husson, and Brusset[19(d)] have found that the metal-oxygen force constants vary as the electronegativity of the metal. Martin[20] has shown, for zinc-blende materials with quite different degrees of covalency, that the bond-stretching force constants vary as $1/r^3$, where r is the interatomic distance. The values of the bond-stretching force constants were, therefore, estimated from the electronegativity of the atoms and their interatomic distances. The force constants were then scaled to fit two constraints; the Cu(2)-O and Y-O stretches are approximately 640 and 190 cm^{-1}, respectively. Although this force field yielded reasonable agreement between the observed and calculated frequencies, the fit was much improved when three interaction force constants (i_1, i_2, and i_3 in Table II) which relate colinear internal-displacement coordinates, were introduced. The negative value of i_1 reflects the high steric repulsion between the two O(2) atoms. Values for the angle-bending force constants and the three interaction force constants were estimated from the normal-coordinate calculations of other metal oxides.[19]

The calculated frequencies and potential energy distribution for orthorhombic $YBa_2Cu_3O_7$ and tetragonal $YBa_2Cu_3O_6$ are given in Table I. The potential energy distribution (PED) gives the relative contribution of the force constants to the potential energy of the normal modes. The forms of the normal modes of the tetragonal form with displacements parallel to the c axis (A_{1g}, B_{1g}, A_{2u}, and B_{2u}) are given in Fig. 2, while those with displacements in the ab plane (E_g and E_u) are given in Fig. 3. The description of the modes is complex, due to the mixing of different internal-displacement coordinates, but a few general statements are possible. The asymmetric O-Cu-O stretches (A_{2u}, E_g, and E_u) all are predicted to have frequencies of $\sim$600–650 cm^{-1}, while the symmetric O-Cu-O stretch (A_{1g}) should have a frequency of $\sim$490 cm^{-1}. Those modes that involve the in-plane bending of the Cu(2)-O(3) chains (E_g and E_u) should have frequencies of $\sim$540 cm^{-1}. Normal modes with frequencies $\sim$350–400 cm^{-1} are predicted to involve the

TABLE II. Force constants for $YBa_2Cu_3O_7$ and $YBa_2Cu_3O_6$.

Force constant	Bond type	$YBa_2Cu_3O_7$ (orthorhombic) Distance (Å)	Value[a]	$YBa_2Cu_3O_6$ (tetragonal) Distance (Å)	Value[a]
C_1	Cu(1)–O(1) [2][b]	1.945	1.52		
C_2	Cu(1)–O(2) [2]	1.827	1.76	1.800	1.82
C_3	Cu(2)–O(3) [4]	1.930	1.55	1.945	1.52
C_3	Cu(2)–O(4) [4]	1.964	1.49	1.945	1.52
C_4	Cu(2)–O(2) [2]	2.332	1.03	2.437	0.95
B_1	Ba–O(1) [4]	2.911	0.55		
B_2	Ba–O(2) [8]	2.753	0.58	2.773	0.58
B_3	Ba–O(3) [4]	2.945	0.54	2.919	0.55
B_3	Ba–O(4) [4]	2.945	0.54	2.919	0.55
Y	Y–O(3) [4]	2.421	0.77	2.397	0.78
Y	Y–O(4) [4]	2.380	0.79	2.397	0.78
CC	Cu(2)–Cu(2) [1]	3.374	0.51	3.315	0.52
BB	Ba–Ba [1]			4.565	0.40
α	O(1)–Cu(1)–O(2) [4]		1.3		
α	O(3)–Cu(2)–O(4) [8]		1.3		1.3
δ	O(2)–Cu(1)–O(2) [2]		0.4		0.4
i_1	Cu(1)–O(2)/Cu(1)–O(2) [1]		−0.15		−0.25
i_2	Cu(1)–O(2)/Cu(2)–O(2) [2]		0.20		0.20
i_3	Ba–O(3)/Y–O(3) [8]		0.10		0.10

[a]Force constant units are stretching; 10^2 N m^{-1} and bending; 10^{-18} N m rad^{-2}.
[b]The number in brackets represents the number of internal coordinates.

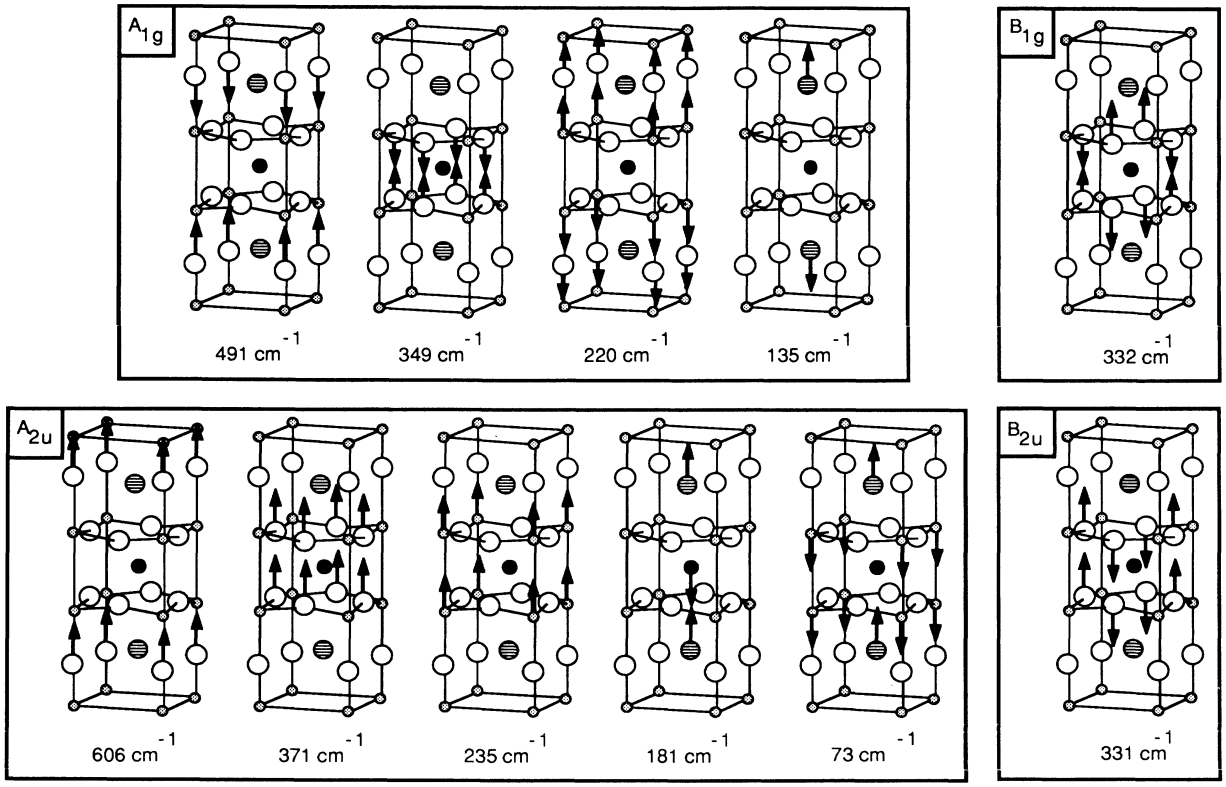

FIG. 2. Normal modes of tetragonal $YBa_2Cu_3O_6$ with displacements parallel to the c axis.

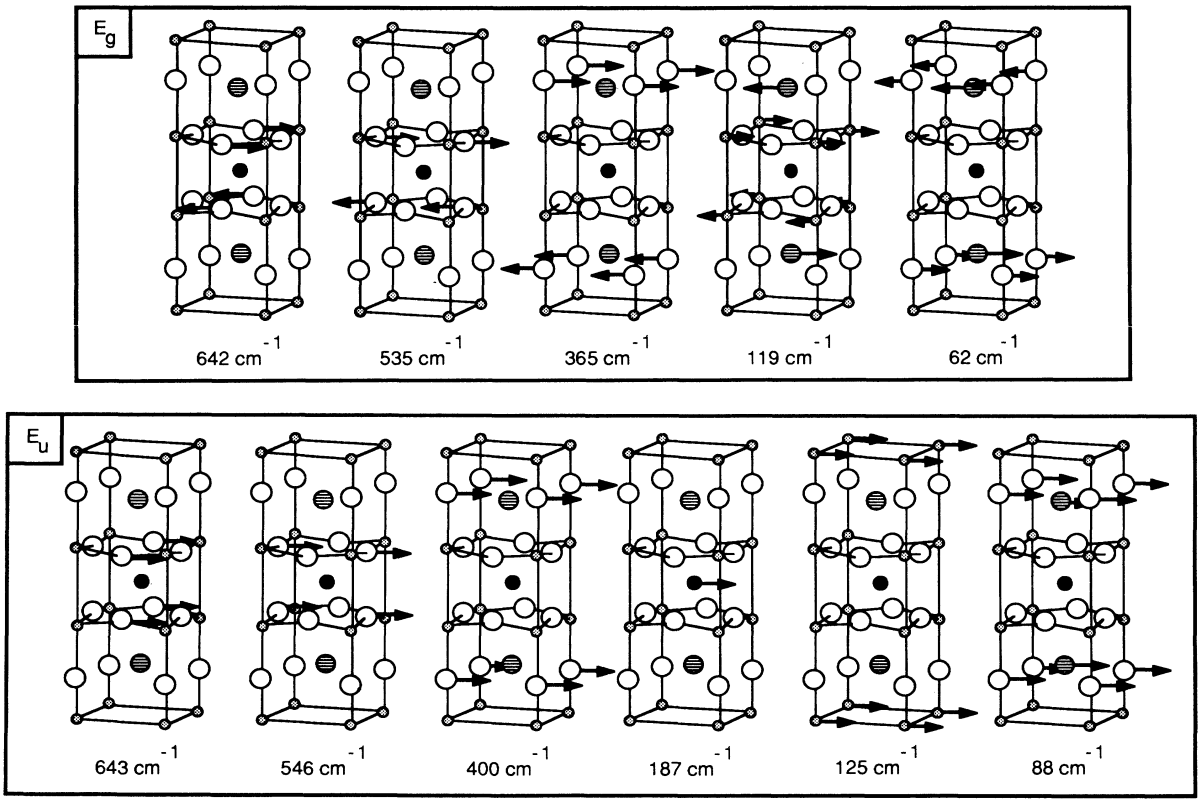

FIG. 3. Normal modes of tetragonal $YBa_2Cu_3O_6$ with displacements in the ab plane.

out-of-plane bending of O(3) in the Cu(2)-O(3)-Cu(2) planes (A_{1g}, B_{1g}, A_{2u}, and B_{2u}) and of O(2) in the Cu(2)-O(2)-Cu(1) chains (E_g and E_u). Motion of the Cu(2)-O(3) planes as a whole should result in normal modes of $\sim$220 cm^{-1} (A_{1g} and A_{2u}). Normal modes involving the motion of yttrium should be at $\sim$185 cm^{-1} (A_{2u} and E_u) while those involving barium and/or copper should be seen below 135 cm^{-1} (A_{1g}, A_{2u}, E_g, and E_u). Normal modes involving the relative displacement of the Ba-O(2) layers are calculated at $\sim$60 and 90 cm^{-1} (E_g and E_u).

Single-crystal Raman studies of the orthorhombic form[8,11,14,25,26] have clearly identified features at 151, 230, 340, 435, and 502 cm^{-1} as due to A_g modes and the feature at 340 cm^{-1} corresponding to the B_{1g} mode of the tetragonal form.[14] As can be seen from Table I, the agreement between the observed and calculated frequencies is very good for all A_g modes except that due to the in-phase motion of O(3) and O(4) out of the Cu(2)-O plane. This mode is calculated to occur at 352 cm^{-1} and is usually assigned[7,11,14] to the observed feature at 435 cm^{-1}. High-pressure Raman studies[27] have recently identified two modes at about 340 cm^{-1} which only become resolved at high pressures, so it is possible that the observed feature at 340 cm^{-1} may in fact be due to the two A_g modes calculated at 332 and 352 cm^{-1}. For the orthorhombic form, two other Raman features are observed.[10,25,26] One at 115 cm^{-1}, which is assigned to the B_{2g} and B_{3g} modes calculated at $\sim$122 cm^{-1}, and one at 550 to 650 cm^{-1}, which is assigned to the higher-frequency B_{2g} and B_{3g} modes calculated to occur at $\sim$530 and 640 cm^{-1}.

For the tetragonal form, the A_g mode at 502 cm^{-1} is predicted (Table I) to decrease in frequency as is found experimentally.[5,10,11,13] This decrease results from the increase in the force constant C_2 being more than offset by a decrease in C_4. The difference in frequency calculated for the lowest A_g and A_{1g} modes is not considered significant as these modes are described in terms of different internal-displacement coordinates. Only one mode of the tetragonal form is predicted to change significantly with oxygen stoichiometry and that is the E_g mode calculated at 365 cm^{-1}. This mode may correspond to the weak Raman feature near 390 cm^{-1} which has been identified as being characteristic of the tetragonal form.[12] One other Raman feature is found to change dramatically with oxygen stoichiometry. The 455 cm^{-1} feature of the tetragonal form is found to soften significantly in the orthorhombic form,[5,10] very much like a very strong B_{1u} mode observed in the infrared spectra at 360 cm^{-1} (see below). An explanation for this is that the 455-cm^{-1} feature results from second-order phonon processes and is a combination band due to the B_{1u} modes that absorb at 360 and 100 cm^{-1}. This would clearly explain the A_g polarization and softening of this mode.

Detailed infrared reflectivity studies[6,7] of the tetragonal form have identified at least nine vibrational features and studies of the samarium isomorph have helped to identify those modes involving the rare earth.[6,7] Above 500 cm^{-1}, there are two observed features, one at 648 cm^{-1} which is assigned to the E_u mode calculated at 643 cm^{-1} and one at 593 cm^{-1} which is assigned to the A_{2u} mode calculated at 606 cm^{-1}. The E_u mode calculated at 546 cm^{-1} may also contribute to the observed 593-cm^{-1} feature. This E_u mode and the A_{2u} mode are both predicted[28] to absorb at lower frequencies in the samarium isomorph as is observed experimentally. The next-lowest frequency feature is observed at 360 cm^{-1} and is assigned to the A_{2u} mode calculated at 371 cm^{-1}. Frequency shifts observed for the samarium compound clearly exclude assignment to the E_u mode calculated at 400 cm^{-1}. The next-four-lowest frequency features are observed at 249, 217, 190, and 147 cm^{-1} and from the frequency shifts observed for the samarium isomorph follows their assignment to modes calculated at 235 (A_{2u}), 187 (E_u), 181 (A_{2u}), and 125 (E_u) cm^{-1}, respectively. The two lowest observed features at 118 and 108 cm^{-1} are then assigned to the calculated modes at 88 (E_u) and 73 (A_{2u}) cm^{-1}.

These normal-coordinate calculations predict some differences in the infrared spectra of the orthorhombic form compared with that of the tetragonal form. Additional features are predicted for the orthorhombic form due to modes calculated at 646 (B_{2u}), 531 (B_{1u}), and 382 (B_{3u}) cm^{-1}, yet only six features at 609, 548, 310, 279, 191, and 151 cm^{-1} have been observed.[29] The three features at 609, 191, and 151 cm^{-1} correspond to features of the tetragonal form and from this follows the assignment of the 609 cm^{-1} feature to the B_{1u} mode calculated to occur at 611 cm^{-1}, the 191-cm^{-1} feature to the B_{1u} mode calculated at 182 cm^{-1}, and the 151-cm^{-1} feature to the B_{2u} and B_{3u} modes calculated to occur at $\sim$159 cm^{-1}. For the tetragonal form, there are no observed features near 550 cm^{-1}; thus, the 548-cm^{-1} feature is assigned to the new B_{1u} mode calculated at 531 cm^{-1}. The 279-cm^{-1} feature is assigned to the B_{1u} mode calculated at 255 cm^{-1}, which is predicted to have a significantly lower frequency in the tetragonal form as is observed experimentally. The remaining unassigned feature at 310 cm^{-1} clearly changes, with decreasing oxygen content, into the tetragonal feature observed at 360 cm^{-1}.[5] However, the calculations clearly indicate that the corresponding B_{1u} mode should have essentially the same frequency for the two forms. The 310-cm^{-1} feature has also been found to undergo an anomalous softening with decreasing temperature[30,31] which has been associated with the superconducting transition.[32] It is herein proposed that there is another effect that can contribute to the apparent softening of this mode in the orthorhombic form, and should also be considered. Transmission spectra of the tetragonal form[33] clearly show the broad nature of this band and undoubtedly some of the breadth is due to overtone and combination bands that gain intensity due to Fermi resonance with the strong A_{2u} mode. The inactive B_{2u} mode cannot interact with this continuum since it does not have the correct symmetry. However, in the orthorhombic form where this mode does have the correct symmetry this inherently weak mode may result in a redistribution of energy levels that results in an absorption minimum or Evans hole.[34] Such effects have been observed clearly in the spectra of solids.[35,36] The loss in absorption intensity is redistributed on either side of the absorption minima and can lead to regions of increased in-

tensity.[34] This effect leads to the prediction of a minimum at ~ 320 cm^{-1} and an increased absorption just to higher frequency of this mode shifting the apparent absorption maximum to lower frequency.

In summary, with the aid of normal-coordinate calculations all of the observed infrared and Raman features of the orthogonal and tetrahedral forms have been assigned. The calculations indicate that the 435-cm^{-1} feature is not due to a first-order A_g mode but is due to second-order processes. For the orthorhombic form, the dominant infrared features are due to the B_{1u} modes; the B_{2u} and B_{3u} modes presumably being masked by the free-carrier absorption. It is suggested that part of the anomalous behavior of the 310-cm^{-1} feature is due in part to the Evans effect[34] which results from the change in symmetry of the inherently weak B_{2u} mode of the tetragonal form.

The author wishes to thank John Eldridge and Chris Homes for many helpful discussions and to acknowledge financial support from the Natural Sciences and Engineering Council (NSERC) of Canada, Strategic Grant No. 5-82032 and Operating Grant No. A5653.

[1]K. Kamarás, C. D. Porter, M. G. Doss, S. L. Herr, D. B. Tanner, D. A. Bonn, J. E. Greedan, A. H. O'Reilly, C. V. Stager, and T. Timusk, Phys. Rev. Lett. **59**, 919 (1987).

[2]M. Stavola, D. M. Krol, W. Weber, S. A. Sunshine, A. Jayaraman, G. A. Kourouklis, R. J. Cava and E. A. Rietman, Phys. Rev. B **36**, 850 (1987).

[3]S. Onari, T. Hiroaki, K. Ohshima, H. Honma, and T. Arai, Solid State Commun. **66**, 303 (1988).

[4]M. Cardona, L. Genzel, R. Lui, A. Wittlin, Hj. Mattausch, F. García-Alvarado, and E. García-González, Solid State Commun. **64**, 727 (1987).

[5]C. Thomsen, R. Lui, M. Bauer, A. Wittlin, L. Genzel, M. Cardona, E. Schonherr, W. Bauhofer, and W. König, Solid State Commun. **65**, 55 (1988).

[6]G. Burns, F. H. Dacol, P. P. Freitas, W. König, and T. S. Plaskett, Phys. Rev. B **37**, 5171 (1988).

[7]C. Thomsen, M. Cardona, W. Kress, R. Liu, L. Genzel, M. Bauer, E. Schonherr, and U. Schröder, Solid State Commun. **65**, 1139 (1988).

[8]G. Burns, F. H. Dalcol, F. Holtzberg, and D. L. Kaiser, Solid State Commun. **66**, 217 (1988).

[9]R. Bhadra, T. O. Brun, M. A. Beno, B. Dabrowski, D. G. Hinks, J. Z. Liu, J. D. Jorgensen, L. J. Nowicki, A. P. Paulikas, I. K. Schuller, C. U. Segre, L. Soderholm, B. Veal, H. H. Wang, J. M. Williams, K. Zhang, and M. Grimsditch, Phys. Rev. B **37**, 5142 (1988).

[10]R. M. Macfarlane, H. J. Rosen, E. M. Engler, R. D. Jacowitz, and V. Y. Lee, Phys. Rev. B **38**, 284 (1988).

[11]D. M. Krol, M. Stavola, W. Weber, L. F. Schneemeyer, J. V. Waszczak, S. M. Zahurak, and S. G. Kosinski, Phys. Rev. B **36**, 8325 (1987).

[12]G. A. Kouroulis, A. Jayaraman, B. Batlogg, R. J. Cava, M. Stavola, D. M. Krol, E. A. Rietman, and L. F. Schneemeyer, Phys. Rev. B **36**, 8320 (1987).

[13]M. Hangyo, S. Nakashima, K. Mizoguchi, A. Fujii, A. Mitsuishi, and T. Yotsuya, Solid State Commun. **65**, 835 (1988).

[14]R. Lui, C. Thomsen, W. Kress, M. Cardona, B. Gegenheimer, F. W. de Wette, J. Prade, A. D. Kulkarni, and U. Schröder, Phys. Rev. B **37**, 7971 (1988).

[15]W. Kress, U. Schröder, J. Prade, A. D. Kulkarni, and F. W. de Wette, Phys. Rev. B **38**, 2906 (1988).

[16]S. L. Chaplot, Phys. Rev. B **37**, 7435 (1988).

[17]P. Brüesch and W. Bührer, Z. Phys. B **70**, 1 (1988).

[18]W. G. McMullan, S. Gygx, and J. C. Irwin, Solid State Commun. **66**, 165 (1988).

[19](a) E. Husson, Y. Repelin, H. Brusset, and A. Cerez, Spectroschim. Acta Part A **35**, 1177 (1979); (b) H. Haeuseler, *ibid.* **37**, 487 (1981); (c) Y. Repelin, E. Husson, N. Q. Dao, and H. Brusset, *ibid.* **35**, 1165 (1979); (d) M. C. Saine, E. Husson, and H. Brusset, *ibid.* **38**, 19 (1982); (e) M. T. Vandenborre, E. Husson and J. L. Fourquet, *ibid.* **38**, 997 (1982).

[20]R. M. Martin, Phys. Rev. B **1**, 4005 (1970).

[21]L. Pauling, Phys. Rev. Lett. **59**, 225 (1988).

[22]F. E. Bates and J. E. Eldrigde, Solid State Commun. **64**, 1435 (1987).

[23]J. E. Greedan, A. H. O'Reilly, and C. V. Stager, Phys. Rev. B **35**, 8843 (1987).

[24]E. B. Wilson, Jr., J. C. Decius, and P. C. Cross, *Molecular Vibrations* (McGraw-Hill, New York, 1955).

[25]V. G. Hadjiev and M. N. Iliev, Solid State Commun. **66**, 451 (1988).

[26]S. L. Cooper, M. V. Klein, B. G. Pazol, J. P. Rice, and D. M. Ginsberg, Phys. Rev. B **37**, 5920 (1988).

[27]K. Syassen, M. Hanfland, K. Strössner, M. Holtz, W. Kress, M. Cardona, U. Schröder, J. Prade, A. D. Kulkarni, and F. W. de Wette (unpublished).

[28]J. E. Eldridge and F. E. Bates, Solid State Commun. (to be published).

[29]D. A. Bonn, J. E. Greedan, C. V. Stager, T. Timusk, M. Doss, S. Herr, K. Kamarás and D. B. Tanner, Phys. Rev. Lett. **58**, 2249 (1987).

[30]A. Wittlin, R. Lui, M. Cardona, L. Genzel, W. König, W. Bauhofer, Hj, Mattausch, A. Simon, and F. García-Alvarado, Solid State Commun. **64**, 477 (1987).

[31]M. Cardona, R. Liu, C. Thomsen, M. Bauer, L. Genzel, W. König, U. Amador, M. Barahona, F. Fernandez, C. Otero, and R. Saez, Solid State Commun. **65**, 71 (1988).

[32]C. Thomsen, R. Liu, A. Wittlin, L. Genzel, M. Cardona, W. König, M. V. Cabanas, and E. Garcia, Solid State Commun. **65**, 219 (1987).

[33]G. Burns, F. H. Dacol, P. Freitas, T. S. Plaskett, and W. König, Solid State Commun. **64**, 471 (1987).

[34]J. C. Evans and N. Wright, Spectrochim. Acta **16**, 352 (1960); J. C. Evans, *ibid.* **16**, 994 (1960); J. C. Evans, *ibid.* **18**, 507 (1961).

[35]M. P. Marzocchi, L. Angeloni, and G. Sbrana, Chem. Phys. **12**, 349 (1976).

[36]J. de Villepin and A. Novak, J. Mol. Struct. **30**, 255 (1970).